ACCOUNTS
of chemical research

Vibrational Spectroscopy of Microhydrated Conjugate Base Anions

KNUT R. ASMIS*,† AND DANIEL M. NEUMARK*,‡,§

†Fritz-Haber-Institut der Max-Planck-Gesellschaft, Faradayweg 4-6, D-14195 Berlin, Germany, ‡Department of Chemistry, University of California, Berkeley, California 94720, United States, and §Chemical Science Division, Lawrence Berkeley National Laboratory, Berkeley, California 94720, United States

RECEIVED ON MARCH 7, 2011

CONSPECTUS

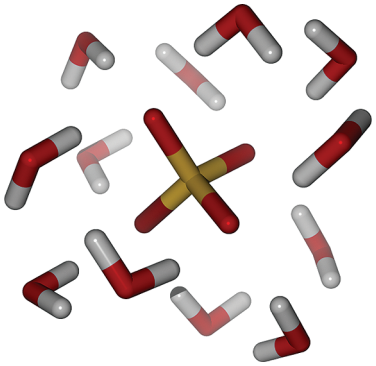

Conjugate-base anions are ubiquitous in aqueous solution. Understanding the hydration of these anions at the molecular level represents a long-standing goal in chemistry. A molecular-level perspective on ion hydration is also important for understanding the surface speciation and reactivity of aerosols, which are a central component of atmospheric and oceanic chemical cycles. In this Account, as a means of studying conjugate-base anions in water, we describe infrared multiple-photon dissociation spectroscopy on clusters in which the sulfate, nitrate, bicarbonate, and suberate anions are hydrated by a known number of water molecules.

This spectral technique, used over the range of 550−1800 cm^{-1}, serves as a structural probe of these clusters. The experiments follow how the solvent network around the conjugate-base anion evolves, one water molecule at a time. We make structural assignments by comparing the experimental infrared spectra to those obtained from electronic structure calculations. Our results show how changes in anion structure, symmetry, and charge state have a profound effect on the structure of the solvent network. Conversely, they indicate how hydration can markedly affect the structure of the anion core in a microhydrated cluster.

Some key results include the following. The first few water molecules bind to the anion terminal oxo groups in a bridging fashion, forming two anion−water hydrogen bonds. Each oxo group can form up to three hydrogen bonds; one structural result, for example, is the highly symmetric, fully coordinated $SO_4^{2-}(H_2O)_6$ cluster, which only contains bridging water molecules. Adding more water molecules results in the formation of a solvent network comprising water−water hydrogen bonding in addition to hydrogen bonding to the anion. For the nitrate, bicarbonate, and suberate anions, fewer bridging sites are available, namely, three, two, and one (per carboxylate group), respectively. As a result, an earlier onset of water−water hydrogen bonding is observed.

When there are more than three hydrating water molecules ($n > 3$), the formation of a particularly stable four-membered water ring is observed for hydrated nitrate and bicarbonate clusters. This ring binds in either a side-on (bicarbonate) or top-on (nitrate) fashion. In the case of bicarbonate, additional water molecules then add to this water ring rather than directly to the anion, indicating a preference for surface hydration. In contrast, doubly charged sulfate dianions are internally hydrated and characterized by the closing of the first hydration shell at $n = 12$. The situation is different for the $^{-}O_2C(CH_2)_6CO^{2-}$ (suberate) dianion, which adapts to the hydration network by changing from a linear to a folded structure at $n > 15$. This change is driven by the formation of additional solute−solvent hydrogen bonds.

Published on the Web 06/15/2011 www.pubs.acs.org/accounts
10.1021/ar2000748

Introduction

Acid molecules undergo dissolution in aqueous media in which they dissociate into two (or more) separately hydrated ions: a proton, and a conjugate base anion. The process of acid dissolution is driven by the ability of the polar water molecules to form hydrogen bonds (HBs) with these ions that are stronger than water–water HBs. The properties of hydrated ions are quite different from those of isolated ions (in the gas phase) or ions in nonpolar media and are governed by the nature of the surrounding hydration network. A molecular-level understanding of ion hydration is thus important, for example, in understanding the surface speciation and reactivity of aerosols, which play a key role in atmospheric and oceanic chemical cycles.[1,2] It is difficult to extract detailed information on the solvent–solute interaction from bulk measurements. Gas phase experiments on size-selected polyatomic anion–solvent complexes, on the other hand, are well-suited for probing how changes in anion structure, symmetry, and charge affect evolution of the solvent shell, one solvent molecule at a time. Gas phase ion vibrational spectroscopy has emerged as one of the most powerful techniques to study the structure and bonding of microsolvated gas phase ions,[3−6] and its application to the study of conjugate anion–water clusters is the primary focus of this Account.

The nitrate, bicarbonate, sulfate, and suberate anions are four prototypical conjugate base anions that are ubiquitous species in aqueous phase chemistry. Nitrate, NO_3^-, is one of the most abundant ionic species in the troposphere and can be formed by rapid acid dissolution of nitric acid in aerosol particles.[7] Bicarbonate, HCO_3^-, plays a central role in the acid–base equilibrium formed when CO_2 is dissolved in water and is thus important in processes such as the pH homeostasis in oceans,[8] the transport of CO_2 between the metabolizing tissues and the lungs,[9] and the regulation of blood pH. Hydrated sulfate dianions, SO_4^{2-}, play a key role in the homogeneous nucleation of ice particles by sulfate aerosols in the upper troposphere[10] and in the regulation of many metabolic and cellular processes.[11] Finally, dicarboxylate dianions such as the suberate dianion, $^-O_2C(CH_2)_6CO_2^-$, are used as building blocks for metal–organic framework materials[12] and are found in aerosol particles comprising photochemical smog.[13] A microscopic, molecular level understanding of the role of hydrated conjugate base anions in these and other processes requires elucidation of the solute–solvent interactions and the precise arrangement of the water molecules comprising the solvation shell.

Important open questions remain regarding the hydration of conjugate base anions at the molecular level. For example, are the anions symmetrically or asymmetrically hydrated in small anion–water clusters and do they prefer interfacial or bulk solvation in larger finite systems? How do the H-bonding motifs depend on the nature and the charge state of the anion, on temperature, and in what way does the HB network influence the geometric structure of the solute? Sulfate and suberate dianions serve as model systems for multiply charged gas phase anions.[14,15] Furthermore, the presence of two charge centers separated by a hydrophobic, aliphatic chain in the suberate dianion is ideal for studying charge-screening and solvent-mediated effects. Previous anion photoelectron spectra in combination with quantum chemical calculations found a delicate dependence of the conformation of dicarboxylate dianions on the degree of hydration and the aliphatic chain length, as well as on temperature.[16−18] Upon addition of a sufficient number of water molecules, the initially quasi-linear dianions change their conformation to a folded structure. A more detailed insight into this solvent-mediated folding mechanism requires structural information, which is challenging to extract from the photoelectron data.

The microhydration studies on nitrate,[19] bicarbonate,[20] sulfate,[21,22] and suberate anions[23,24] described here complement the pioneering work on microhydrated conjugate base anions by Kebarle and co-workers,[25] who used electrospray ionization mass spectrometry to determine free energies of hydration, and the experiments by Wang and co-workers,[26−28] who applied anion photoelectron spectroscopy to characterize their electronic and geometric structure. Vibrational spectroscopy allows for a more detailed insight into the solute–solvent and solvent–solvent interactions, in particular the structure of the first hydration shell. With the aid of electrospray sources, conjugate base anions can be transferred efficiently and without fragmentation from a solution into the gas phase. Careful adjustment of the source conditions allows control over the degree of hydration of these ions, from the bare ion to ions with many water molecules. With the help of mass filters, size-selected ions with a well-defined number of water molecules can then be isolated, manipulated, and spectroscopically probed.

Gas Phase Ion Spectroscopy

When working with mass-selected ions in the gas phase, the attainable ion number densities are small, typically below $\sim 10^8$ ions/cm^3 due to space charge effects. This low density prohibits the application of most of the powerful

techniques developed for condensed phase measurements. For example, consider direct absorption, which take advantages of the Beer–Lambert law,

$$I(\nu) = I_0(\nu)\, e^{-\sigma(\nu)nl} \quad (1)$$

in which a light beam of intensity I_0 is attenuated by $1 - (I/I_0)$ after it passes through a probe with an absorption cross section σ, number density n, and length l. As the number density is lowered, it becomes increasingly difficult to detect these minute changes in intensity. For typical values of σ, n, and l of 10^{-17} cm^2, 10^7 cm^{-3}, and 10 cm, the attenuation is only 10^{-9}. Therefore, alternative methods have been developed, in which the absorption of photons is measured indirectly. These techniques detect the response of the molecule or ion after photon absorption, which could be a change in quantum state, mass, or charge, accompanied by photon emission, fragmentation, or photoelectron ejection, and hence are generally referred to as action spectroscopy. The formalism describing action spectroscopy remains nearly identical to eq 1, except that the light intensity I_0 is replaced by the number molecules/ions N_0 and the term nl by the laser fluence F:

$$N(\nu) = N_0(\nu)\, e^{-\sigma(\nu)F} \quad (2)$$

Among the different types of action spectroscopies, infrared multiple photon dissociation (IRMPD) spectroscopy, paired with quantum chemistry, has emerged as one of the most efficient and generally applicable approaches to structural investigation of microhydrated ions in the gas phase. Photodissociation techniques have the advantage that fragment ions can be detected background-free and with nearly 100% detection efficiency. High selectivity can be achieved through mass selection of parent and fragment ions using appropriate mass filters.

IRMPD Spectroscopy. An IRMPD spectrum is measured by irradiating ions with IR radiation and monitoring the yield of parent and/or fragment ions as a function of the irradiation wavelength. In order to induce fragmentation, the hydrated parent ion $M^-(H_2O)_n$ is required to absorb sufficient energy to overcome the (lowest) dissociation threshold:

$$M^-(H_2O)_2 \xrightarrow{m \cdot h\nu} M^-(H_2O)_{n-1} + H_2O \quad (3)$$

Process 3 typically requires the absorption of several photons, since excitation of fundamental vibrational transitions typically does not deposit sufficient energy to induce dissociation. The absorption mechanism and efficiency depend strongly on the size and properties of the absorbing species, its initial internal energy, and the properties of the light source.[29] The mechanism of IRMPD for polyatomic molecules can be conceptually divided into three regimes:[30] (1) the polyatomic molecule is excited resonantly over discrete states into the quasi-continuum region, (2) the molecule continues to absorb photons resonantly, but this energy is quickly randomized among all vibrational degrees of freedom, and (3) once the internal energy reaches the dissociation limit, the molecule dissociates according to the statistical model of unimolecular reactions. An important role is played by anharmonicities. First, they prevent the absorption of more than a few photons in a single mode, as the anharmonicity will usually shift the resonance out of the excitation range of the laser ("anharmonic bottleneck"). Second, anharmonicities introduce a coupling mechanism between different modes, which allows for an internal vibrational redistribution (IVR) of the energy. With increasing internal energy E_i, the density of rovibrational states $\sigma(E_i)$ increases very rapidly, roughly proportional to E_i^N, where N is the number of vibrational degrees of freedom. In the limit of fast IVR, each photon absorption event is followed by redistribution of the energy, effectively "de-exciting" the IR-excited vibrational mode and accessing the quasi-continuum by absorption of a single photon. In such cases, the IRMPD spectrum then often resembles the linear absorption spectrum. This is particularly important for assigning structures based on quantum computational predictions, since standard computational tools only give direct access to calculating linear absorption spectra, generally within the harmonic approximation, but are difficult to extend to the multiple absorption case.

Experimental Realization

The IRMPD experiments are carried out on an ion trap–tandem mass spectrometer[23,31] similar to that shown in Figure 1. They require widely tunable, sufficiently high fluence IR radiation and can currently only be performed at IR free electron laser facilities; commercially available table-top laser systems generally lack sufficient fluence to drive IRMPD over a wide IR frequency range. For the experiments

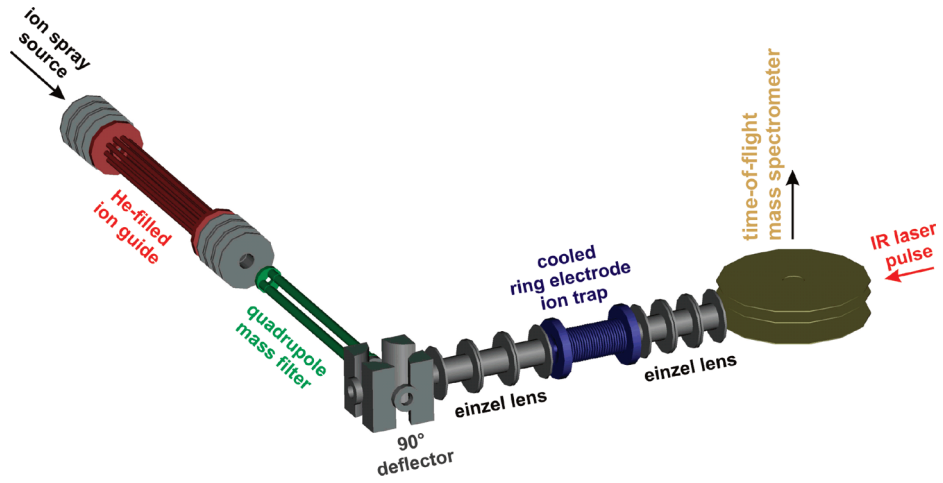

FIGURE 1. Schematic of the ion trap–tandem mass spectrometer. The continuous beam of negative ions from an electrospray source is collimated in an ion guide and mass-selected in a quadrupole mass filter. Mass-selected ions are deflected by 90° and continuously loaded in the buffer gas-filled (He) ring electrode ion trap held at 10–15 K. Prior to the firing of the IR laser pulse, the cooled ions are extracted from the ion trap and focused into the extraction region of an orthogonally mounted TOF mass spectrometer. Here, the ion packet is temporally and spatially overlapped with the IR photodissociation laser pulse and the depletion of the parent ions, as well as the formation of photofragment ions, is simultaneously monitored by way of TOF mass spectrometry.

discussed here, the spectrometer is temporarily installed at the "Free Electron Laser for Infrared eXperiments" (FELIX) user facility[32] in the FOM Institute Rijnhuizen (The Netherlands). Microhydrated conjugate base anions are produced by an electrospray source and transferred into the high vacuum system. Ions of interest are mass-selected in a quadrupole mass filter and focused into a linear radio frequency ion trap. The ion trap is filled with He buffer gas and cooled to cryogenic temperatures by means of a closed cycle He cryostat. Collisions with the He buffer gas cool the ions close to the ambient temperature. IRMPD spectra are obtained by accumulating and cooling ions in the ion trap, extracting them into the extraction region of a time-of-flight (TOF) mass spectrometer, and irradiating them with pulsed radiation from FELIX prior to the measurement of the TOF mass spectra. FELIX macropulses are produced at 5 or 10 Hz with a pulse length of up to 7 μs, a bandwidth of the laser wavelength over the range from 550 to 1800 cm^{-1} of ca. 0.3% rms, and typical pulse energies of up to 50 mJ. The experiments on microhydrated sulfate dianions were performed on an earlier version of the ion trap–tandem mass spectrometer[33] under slightly different conditions.[21]

Binding Motifs in Conjugate Anion–Water Clusters

Nitrate–Water Clusters: Solvent-Induced Symmetry Breaking. Bare NO_3^- is planar and has three equivalent N–O bonds. Of the six vibrational degrees of freedom, only the degenerate ν_3 (e′) antisymmetric stretching vibration is IR active with significant intensity, resulting in a single band at 1349 cm^{-1} in the gas phase IR spectrum.[34] In aqueous media, solvent as well as counterion interactions are sufficiently strong to perturb the electronic structure of NO_3^-, distorting the anion from D_{3h} symmetry of the bare anion, lifting the degeneracy of its vibrational transitions, and rendering all six vibrational modes both Raman and IR-active.[35–37]

IRMPD spectra of $NO_3^-(H_2O)_n$ clusters[19] with $n = 1–6$ are shown in Figure 2. Most spectra show a pair of peaks centered around 1350 cm^{-1} (labeled A in Figure 2) and a weaker band around 1660 cm^{-1} (labeled B in Figure 2). Features A and B correspond to the NO_3^- antisymmetric stretching mode ν_3 and the water bending modes, respectively. Little or no signal is observed below 1200 cm^{-1}, where the water librational modes are expected. The most striking feature in the experimental IRMPD spectra is the variation of the ν_3 splitting (feature A) with size, which represents a sensitive probe of the hydration environment. For $n = 3$, no splitting and only a minor shift compared to the $NO_3^- \cdot$Ar data[34] is observed, signaling a hydration shell of high symmetry. In contrast, the spectra for $n = 2$ and $n = 5$ show relatively large splittings (>40 cm^{-1}), indicating significantly more asymmetric hydration. Interestingly, the shift observed in the condensed phase data is even larger, in the range from 60 to 70 cm^{-1}, suggesting that the asymmetric hydration persists in solution.[35,36]

The evolution of the position and solvation-induced splitting of the ν_3 band with the number of water molecules

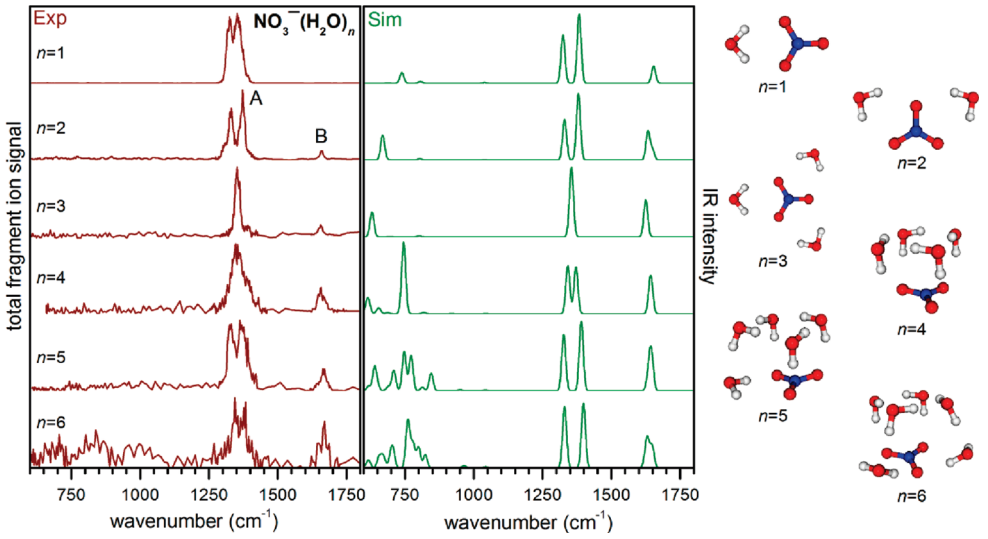

FIGURE 2. Experimental IRMPD (left) and simulated IR (right) spectra of $NO_3^-(H_2O)_n$ ions with $n = 1-6$. The total fragment ion yield is plotted as a function of the photon energy (cm^{-1}). The simulated spectra are derived from B3LYP/aug-cc-pVDZ scaled harmonic frequencies and intensities and convoluted using a Gaussian line shape function with a fwhm of 15 cm^{-1}.[19]

in the cluster are reproduced rather well by the scaled harmonic frequencies, calculated using density functional theory, of the lowest energy structures shown in Figure 2, suggesting that our calculated structural motifs are reasonable. The minimum energy structures are similar to those found previously, but for $n = 3$ and $n = 6$ a different energetic ordering of the isomers is found.[38] Low energy bands, in particular those due to excitation of water librational modes, whose vibrational frequencies depend sensitively on the nature of the HB network, are not observed in the experimental spectra. These are difficult to detect in IRMPD experiments, because IVR results in HB breaking before enough photons are absorbed to dissociate the ion.

Based on the comparison between experimental and simulated IR spectra, several key trends are identified. The first three water molecules bind to the nitrate ion in a bidentate fashion, keeping the planar symmetry of the bare ion. Consequently, the ground state structure of the $n = 3$ isomer does not contain a ring of three water molecules, as predicted previously.[38] Breaking of the planar symmetry and the onset of extensive water–water H-bonding is observed starting with $n = 4$. A ring of four water molecules singly H-bonded to each other is particularly stable and found as a structural motif in all of the larger, most stable clusters. In these larger clusters, the maximum number of HBs to the ionic core is maintained, while any remaining water O–H bonds favor an orientation which maximizes the number of interwater HBs. Up to $n = 6$, all water molecules directly bind to the nitrate ion, that is, comprise the first hydration shell. Isomers containing free O–H bonds and water molecules in the second hydration shell are found to lie higher in energy. The $n = 6$ isomer is not highly symmetric as predicted previously;[39,40] the splitting in the ν_3 band clearly supports a lower-symmetry structure, probably of C_1 symmetry. Our results thus suggest that nitrate ions prefer surface solvation at small cluster sizes. This is confirmed by recent molecular dynamics (MD) simulations, which show that surface structures are preferred over internally solvated ones for clusters containing less than 300 water molecules.[41]

Bicarbonate–Water Clusters: Surface Solvation. IRMPD spectra of $HCO_3^-(H_2O)_n$ clusters[20] were measured up to $n = 10$, and those with $n = 1-8$ are shown in Figure 3. The six bands observed in the IRPMD spectra can be readily assigned based on the IR spectrum of HCO_3^- in bulk water,[42] shown in Figure 4, and calculated vibrational frequencies of the bare and solvated anion. The small peaks B and C are assigned to the CO_3 out-of-plane mode and C–OH stretching mode, respectively. Peak D is assigned to the COH bending mode, while the more intense peak E is assigned to the CO_2 symmetric stretch. Peaks F and G are assigned to the CO_2 antisymmetric stretch of the anion core as well as the various water bending modes.[43] Finally, peak A is located in the region where the CO_2 bending mode is expected. However, this mode has very weak IR absorption[42] and thus band A is instead assigned to the various water librational modes.[43]

We performed electronic structure calculations on the $n = 1-8$ species to determine the structure of the lowest-lying

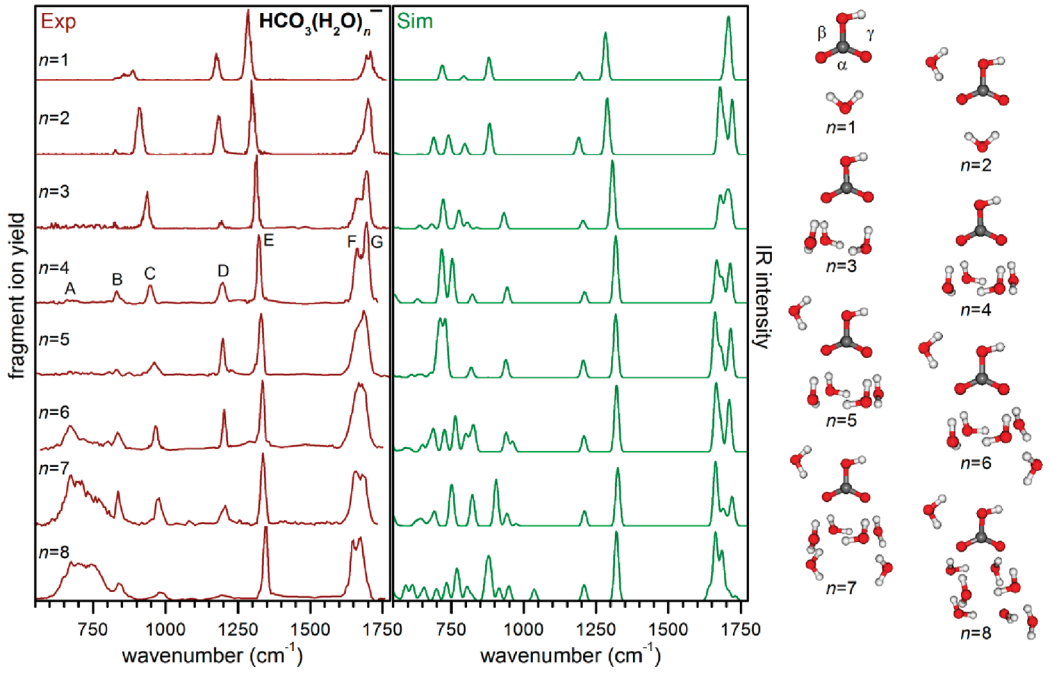

FIGURE 3. Experimental IRMPD (left) and simulated IR (right) spectra of $HCO_3^-(H_2O)_n$ ions with $n = 1-8$. The total fragment ion yield is plotted as a function of the photon energy (cm^{-1}). The simulated spectra are derived from MP2/6-311+G(d,p) scaled harmonic frequencies and intensities and convoluted using a Gaussian line shape function with a fwhm of 15 cm^{-1}.[20]

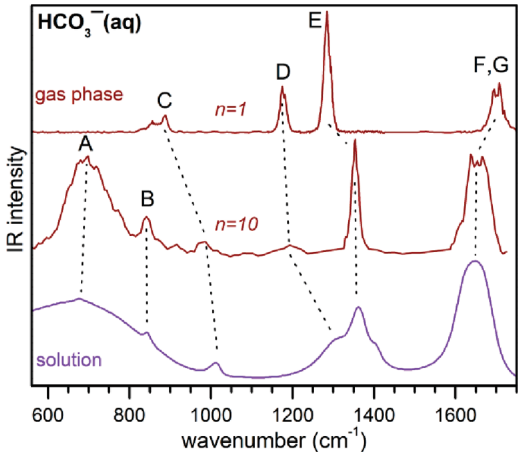

FIGURE 4. Comparison of the gas phase IRMPD spectra of $HCO_3^-(H_2O)_n$ with $n = 1$ and $n = 10$ and the room-temperature IR spectrum of an aqueous $KHCO_3$ solution.[42]

isomers (see Figure 3).[20] Comparison of the experimental and calculated IR spectra does not always enable unambiguous identification of a single isomer for each cluster. Nonetheless, the overall good agreement between the calculated spectra and experiment allows us to determine general trends in the stepwise solvation motifs of the HCO_3^- anion. The most important of these is the strong preference of water molecules to bind to the negatively charged CO_2 moiety (the α site; see Figure 3). A maximum of four waters can directly interact with the anion at this position. The binding motif in the most stable isomer of $n = 4$, which consists of a four-membered ring with each water forming a single HB with the CO_2 moiety, is retained in all the most stable isomers of the larger clusters. Starting at $n = 6$, the additional solvent molecules form a second hydration shell, extending the water−water network located at the α site of the bicarbonate anion. Up to $n = 8$, the water molecules remain located within or close to the plane of the bicarbonate anion. Isomers with water located on top of the HCO_3^- core, like in $NO_3^-(H_2O)_{4-6}$ (see Figure 2), were significantly higher in energy. Bands due to water librational modes (labeled as peak A in the larger clusters) are not observed in the experimental spectra for clusters with $n < 6$ and their absence originates from similar effects as discussed above. Clusters with $n \geq 6$ all contain water molecules in the second hydration shell, leading to a significant lowering of the cluster dissociation energy and appearance of the water librational bands in their IRMPD spectra.

The comparison of the IRMPD spectra for $n = 1$ and $n = 10$ to the IR spectrum of aqueous bicarbonate, shown in Figure 4, nicely illustrates that all absorption features, with the exception of peak D, have nearly converged to the condensed phase limit for $n = 10$. Note that the peak widths in the room temperature IR spectrum result from thermal broadening, which is nearly absent in the IRMPD spectra measured at 12 K. Peak D is associated with the COH

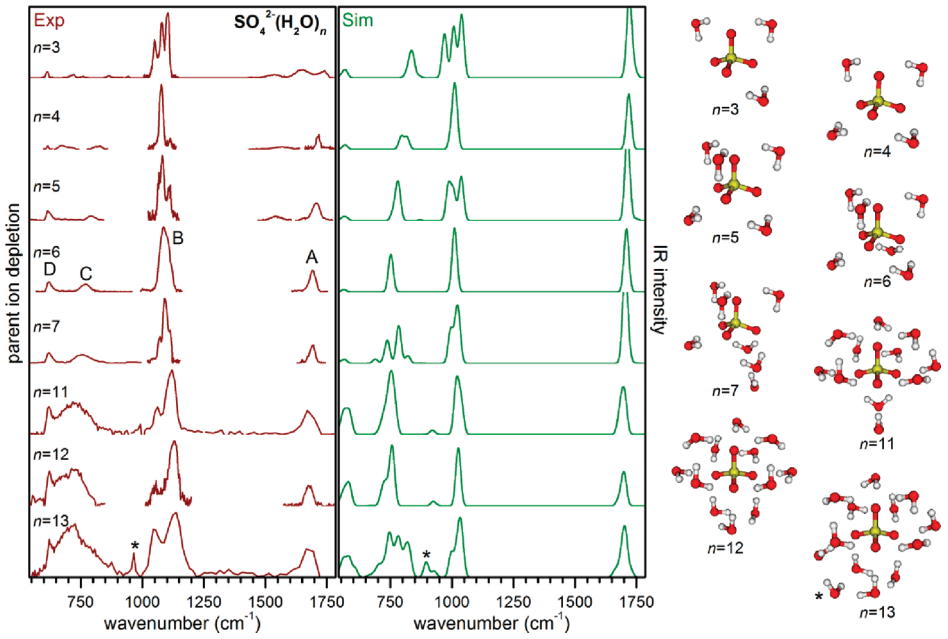

FIGURE 5. Experimental IRMPD (left) and simulated IR (right) spectra of $SO_4^{2-}(H_2O)_n$ ions with $n = 1-7$ and $n = 11-13$. The parent ion depletion is plotted as a function of the photon energy (cm^{-1}). The simulated spectra are derived from B3LYP/TZVP scaled harmonic frequencies and intensities and convoluted using a Gaussian line shape function with a fwhm of 20 cm^{-1}.[21]

bending mode of the hydroxyl group of HCO_3^-. The absence of a significant shift of peak D from $n = 1$ to $n = 10$ indicates that binding of a water molecule to the γ site (see Figure 3) is disfavored for all clusters studied here. While the HCO_3^- anion thus retains its C_s (planar) symmetry up to $n = 10$ in the gas phase, it is known from solution phase Raman spectra[42,44] that completely hydrated HCO_3^- anions have C_1 symmetry. However, a HCO_3^- core of C_1 symmetry is predicted for isomers with a water molecule bound in the γ position, and consequently, a nonplanar HCO_3^- anion is expected for larger water clusters.

Sulfate–Water Clusters: Internal Solvation. IRMPD spectra of $SO_4^{2-}(H_2O)_n$ clusters[21] were measured up to $n = 24$ and selected spectra with up to $n = 13$ are displayed in Figure 5. There are four bands that appear prominently in the spectra, labeled A–D in Figure 5. In solution, the tetrahedrally symmetric sulfate dianion has two IR active modes: the antisymmetric stretching and bending modes at 1106 and 617 cm^{-1}, respectively.[45] These modes are assigned to the bands labeled B and D, which fall in the ranges 1080–1110 and 615–626 cm^{-1}, respectively. The IR spectrum of liquid water[43] also exhibits two bands in this spectral region: the intramolecular bending modes at 1644 cm^{-1} and the librational modes at 683 cm^{-1}. Accordingly, these modes are assigned to bands A and C, which occur between 1735–1674 and 864–681 cm^{-1}, respectively, in the IRMPD spectra.

The splitting pattern of band B provides a key point of comparison. The antisymmetric stretching mode assigned to this band is triply degenerate for a free sulfate ion with T_d symmetry, so the shape of this band provides a sensitive probe of the local solvent environment. The calculated spectra show that band B is quite strongly split for the low-symmetry C_2 $n = 3$ structure, where the solvation of the sulfate O-atoms is quite anisotropic. This splitting disappears for the isotropically solvated and highly symmetric D_{2d} $n = 4$ and T_d $n = 6$ structures, where each of the sulfate O-atoms accept 2 and 3 HBs, respectively. The C_{2v} symmetry $n = 5$ structure is an intermediate case, exhibiting a smaller splitting than $n = 3$, corresponding to a less anisotropic solvation environment.

For the smaller sizes ($n = 3-6$), each water adds to an open edge of the sulfate tetrahedron in a "bridging" fashion, forming HBs to adjacent sulfate O-atoms. However, for $n \geq 4$, at least three isomers, including two which contain water–water HBs, lie within less than 10 kJ/mol[46] and the latter two are entropically favored, such that they are preferentially populated at higher temperatures.[46,47] The solvation shell can contain a maximum of six bridging waters, and the formation of water–water HBs becomes competitive with bridging ligands in this size range. The $n = 12$ structure represents a complete shell-closing, with each oxygen atom in the sulfate accepting three HBs. This conclusion is supported by the appearance of a new band in the spectra of the

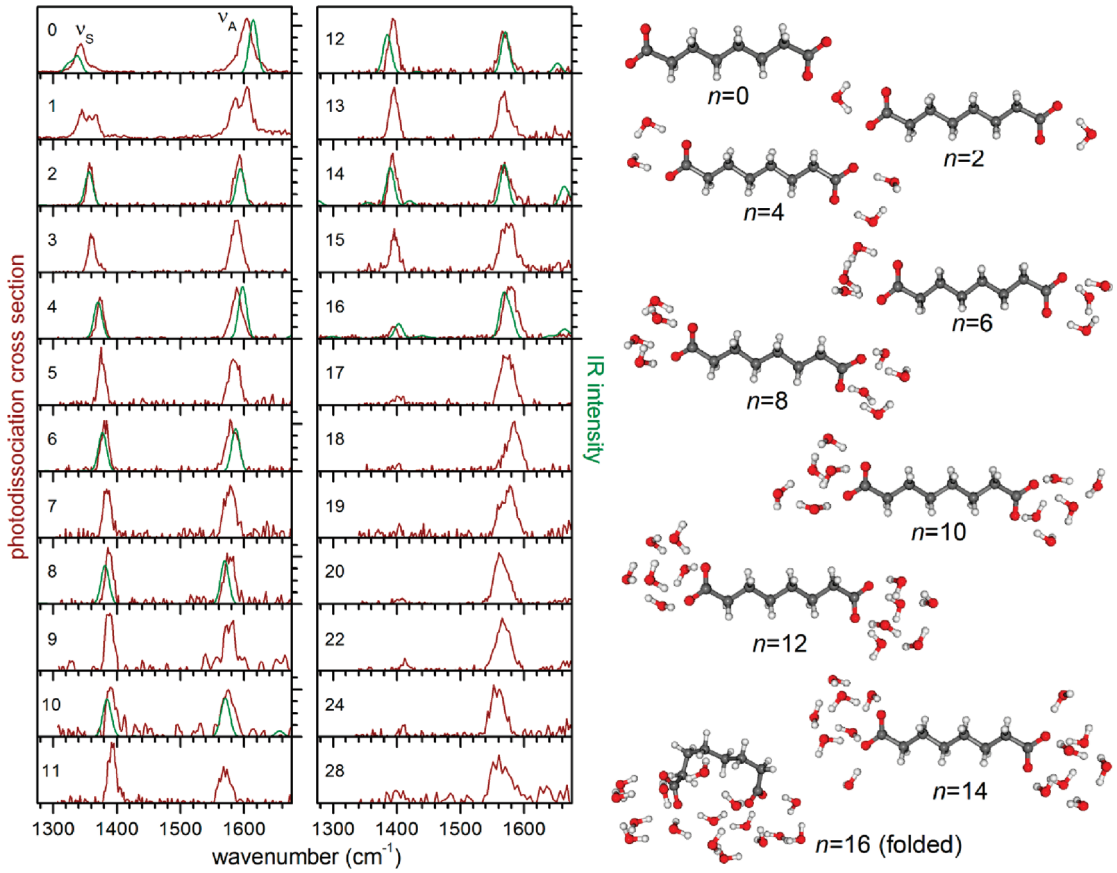

FIGURE 6. Experimental IRMPD spectra (red) of $SA^{2-}(H_2O)_n$ clusters with $n = 0-28$ in the region of the ν_S and ν_A carboxylate stretching modes. The photodissociation cross section is plotted as a function of the photon energy (cm^{-1}). The spectra for $n = 0$ and $n = 1$ are taken from ref 23. Simulated linear IR absorption spectra (green) and optimized geometries are shown for $n = 0$, 2, ..., 16.[24]

$n = 13$ clusters (band marked with an asterisk (∗) in Figure 5), which is associated with the vibration of the water molecule in the second solvation shell. Thus, in contrast to nitrate and bicarbonate, sulfate dianions prefer to be internally hydrated.

Suberate–Water Clusters: Solvent-Mediated Folding. In order to gain more detailed insight into the solvent-mediated folding mechanism observed in microhydrated dicarboxylate dianions,[17] we measured vibrational spectra of microhydrated suberate dianions (SA^{2-}) with up to 28 water molecules.[24] An initial study on $SA^{2-}(H_2O)_{0-2}$ showed that, of the various IR-active modes, the carboxylate stretching bands represent the most sensitive probe for solute–solvent interactions, in contrast to, for example, the O–H and C–H stretching bands which are broadened due to the fluctionality of this particular system already at low internal temperatures.[23]

IRMPD spectra of $SA^{2-}(H_2O)_n$ clusters with $n = 0$ to $n = 28$ are shown in the spectral region of the carboxylate stretching modes (1300–1650 cm^{-1}) in Figure 6. The two terminal carboxylate groups yield two symmetric (ν_S) and two antisymmetric (ν_A) stretching modes. Each pair of modes is only weakly coupled, due to the large separation between the two carboxylate groups, and two bands are observed for $n = 0$. The first water molecule binds asymmetrically to one of the carboxylate groups, splitting each band into its two components ($n = 1$ spectrum in Figure 6). For larger clusters, the widths of the ν_S and ν_A bands narrow again, suggesting that the dianion is symmetrically hydrated by alternatively adding a water molecule to one of the two carboxylate groups. This is confirmed by the nearly monotonic, gradually decreasing shifts of the ν_S band to higher and the ν_A band toward lower energies with increasing n. However, the frequencies of aliphatic dicarboxylate dianions in bulk solution are reached only for ν_S but not for ν_A, suggesting that the latter is more sensitive to longer range effects.

The behavior of the band intensities shows a more pronounced size dependence. This is best seen for the IRMPD spectra of $n \geq 14$, where the intensity of the ν_S band drops significantly at $n = 16$ and remains low throughout the

spectra of the larger clusters. To elucidate the origin of this behavior, we determined the minimum energy structures for even n up to $n = 16$ and derived IR spectra (see Figure 6) from calculated harmonic vibrational frequencies and IR intensities.[24] The bare dianion assumes a quasi-linear geometry due to the electrostatic repulsion of the two terminal carboxylate groups. As water molecules are added to the complex, the two carboxylate groups are symmetrically hydrated, effectively shielding the charge centers, but keeping the quasi-linear geometry. Starting with $n = 12$, stable, folded geometries are also found. Moreover, all simulated IR spectra of the folded geometries show a strong reduction in intensity of the IR-active ν_S mode, whereas the ν_A mode remains strong and decoupled, like in the linear configuration. This trend is independent of the particular structure of the solvent network.

The IR spectra thus support the previous anion photoelectron spectroscopy studies, which reported a transition from linear to folded structures to occur at $n = 16$.[17,18] In addition, the intensity of the ν_S mode represents a sensitive probe to distinguish between linear and folded dicarboxylate dianions, because this mode strongly responds to the coupling between the carboxylate group and the saturated chain. In contrast, the frequencies of the carboxylate stretching modes are more sensitive to the local H-bonding network. Interestingly, our quantum chemical calculations show that the stabilization of the folded dianion structures is essentially due to the formation of additional *solute–solvent* rather than solvent–solvent HBs.[24] Therefore, the folded structures should also persist in much larger microhydrated clusters, as is confirmed by molecular dynamics simulations involving 1400 water molecules, which show that suberate dianions prefer bent, surface solvated structures.[16]

Concluding Remarks

These results show that IRMPD spectroscopy is a powerful tool for identifying typical binding motifs in hydrated conjugate base anions, one water molecule at a time. The position and intensity of the vibrational modes of the solute anion, in particular the oxo stretching and bending modes, represent sensitive probes for the geometry of the anion as well as the nature of the hydration network. In contrast, the vibrational signature of the inter- and intramolecular modes associated with the water molecules are more challenging to interpret. The inherent fluctionality of these modes typically leads to broader, unresolved bands that are difficult to assign on the basis of electronic structure calculations and generally requires the use of computationally more demanding molecular dynamics simulations.

Three of the systems chosen here, the nitrate (NO_3^-), bicarbonate (HCO_3^-), and sulfate (SO_4^{2-}) anions, show how hydration of polyatomic anions depends sensitively on their structure and charge state. For example, the nitrate and bicarbonate anions are of similar size, but the lower symmetry of bicarbonate leads to a very different hydration pattern, with addition of waters at the OH site strongly disfavored. Comparison of the sulfate dianion clusters with nitrate and bicarbonate clusters shows that the additional anionic charge favors structures that maximize hydrogen-bonding interactions with the anionic core over water–water hydrogen bonding. The results on the suberate anions exemplify how hydration can have a major structural effect on a core anion, a result that may have implications in the hydration of charged biomolecules.

BIOGRAPHICAL INFORMATION

Knut R. Asmis received his Dr. rer. nat. in Physical Chemistry from the Université de Fribourg, Switzerland, in 1996. After his postdoctoral fellowship at the University of California, Berkeley, he moved to the Freie Universität Berlin in 1999 and earned his Habilitation in Experimental Physics in 2006. Since 2005 he is a Research Group Leader and since 2009 a Permanent Staff Scientist at the Fritz-Haber-Institut of the Max-Planck-Gesellschaft in Berlin, where he continues to develop new techniques to study the vibrational spectroscopy of gas phase clusters, with emphasis on hydrogen bonding, ion and electron solvation, as well as the structure, dynamics, and reactivity of metal oxide clusters.

Daniel M. Neumark is Professor of Chemistry at the University of California, Berkeley, where he is currently Department Chair, and is a Faculty Senior Scientist in the Chemical Sciences Division of Lawrence Berkeley National Laboratory. His research interests focus on using photoelectron spectroscopy to probe reaction and cluster dynamics. His awards include Alfred P. Sloan Fellow (1989), Camille and Henry Dreyfus Teacher-Scholar (1991), Fellow, American Physical Society (1993), Fellow, American Association for the Advancement of Science (1994), Fellow of the American Academy of Arts and Sciences (2000), American Chemical Society Nobel Laureate Signature Award (with Martin Zanni) (2000), Bomem-Michelson Award (2001), William F. Meggers Award (2005), Irving Langmuir Award (2008), Dudley Herschbach Medal (2009), and ACS Fellow (2010).

We thank the Stichting voor Fundamenteel Onderzoek der Materie (FOM) for beam time and the staff for support and assistance. This research is funded by the European Community's Seventh Framework Programme (FP7/2007–2013) Grant No. 226716, and by the Air Force Office of Scientific Research under Grant No. F49620-03-1-0085.

FOOTNOTES

*To whom correspondence should be addressed. E-mail: asmis@fhi-berlin.mpg.de, dneumark@berkeley.edu.

REFERENCES

1 Prather, K. A.; Hatch, C. D.; Grassian, V. H. Analysis of Atmospheric Aerosols. *Annu. Rev. Anal. Chem.* **2008**, *1*, 485–514.

2 Jungwirth, P.; Tobias, D. J. Specific Ion Effects at the Air/Water Interface. *Chem. Rev.* **2006**, *106*, 1259–1281.

3 Okumura, M.; Yeh, L. I.; Lee, Y. T. The Vibrational Predissociation Spectroscopy of Hydrogen Cluster Ions. *J. Chem. Phys.* **1985**, *83*, 3705–3706.

4 Lisy, J. M. Spectroscopy and Structure of Solvated Alkali-Metal Ions. *Int. Rev. Phys. Chem.* **1997**, *16*, 267–289.

5 Duncan, M. A. Frontiers in the Spectroscopy of Mass-Selected Molecular Ions. *Int. J. Mass. Spectrom.* **2000**, *200*, 545–569.

6 Robertson, W. H.; Johnson, M. A. Molecular Aspects of Halide Ion Hydration: The Cluster Approach. *Annu. Rev. Phys. Chem.* **2003**, *54*, 173–213.

7 Finlayson-Pitts, B. J. The Tropospheric Chemistry of Sea Salt: A Molecular-Level View of the Chemistry of NaCl and NaBr. *Chem. Rev.* **2003**, *103*, 4801–4822.

8 Caldeira, K.; Wickett, M. E. Anthropogenic Carbon and Ocean pH. *Nature* **2003**, *425*, 365–365.

9 Silverman, D. N.; Lindskog, S. The Catalytic Mechanism of Carbonic-Anhydrase - Implications of a Rate-Limiting Protolysis of Water. *Acc. Chem. Res.* **1988**, *21*, 30–36.

10 Ramanathan, V.; Crutzen, P. J.; Kiehl, J. T.; Rosenfeld, D. Atmosphere - Aerosols, Climate, and the Hydrological Cycle. *Science* **2001**, *294*, 2119–2124.

11 Lee, A.; Dawson, P. A.; Markovich, D. NaS_i-1 and Sat-1: Structure, Function and Transcriptional Regulation of Two Genes Encoding Renal Proximal Tubular Sulfate Transporters. *Int. J. Biochem. Cell Biol.* **2005**, *37*, 1350–1356.

12 Rao, C. N. R.; Natarajan, S.; Vaidhyanathan, R. Metal Carboxylates with Open Architectures. *Angew. Chem., Int. Ed.* **2004**, *43*, 1466–1496.

13 Grosjean, D.; Vancauwenberghe, K.; Schmid, J. P.; Kelley, P. E.; Pitts, J. N. Identification of C_3-C_{10} Aliphatic Dicarboxylic-Acids in Airborne Particulate Matter. *Environ. Sci. Technol.* **1978**, *12*, 313–317.

14 Wang, L. S.; Ding, C. F.; Wang, X. B.; Nicholas, J. B.; Nicholas, B. Probing the Potential Barriers and Intramolecular Electrostatic Interactions in Free Doubly Charged Anions. *Phys. Rev. Lett.* **1998**, *81*, 2667–2670.

15 Wang, X. B.; Wang, L. S. Photoelectron Spectroscopy of Multiply Charged Anions. *Annu. Rev. Phys. Chem.* **2009**, *60*, 105–126.

16 Minofar, B.; Mucha, M.; Jungwirth, P.; Yang, X.; Fu, Y. J.; Wang, X. B.; Wang, L. S. Bulk Versus Interfacial Aqueous Solvation of Dicarboxylate Dianions. *J. Am. Chem. Soc.* **2004**, *126*, 11691–11698.

17 Yang, X.; Fu, Y. J.; Wang, X. B.; Slavicek, P.; Mucha, M.; Jungwirth, P.; Wang, L. S. Solvent-Mediated Folding of a Doubly Charged Anion. *J. Am. Chem. Soc.* **2004**, *126*, 876–883.

18 Wang, X. B.; Yang, J.; Wang, L. S. Observation of Entropic Effect on Conformation Changes of Complex Systems under Well-Controlled Temperature Conditions. *J. Phys. Chem. A* **2008**, *112*, 172–175.

19 Goebbert, D. J.; Garand, E.; Wende, T.; Bergmann, R.; Meijer, G.; Asmis, K. R.; Neumark, D. M. Infrared Spectroscopy of the Microhydrated Nitrate Ions $NO_3^-(H_2O)_{1-6}$. *J. Phys. Chem. A* **2009**, *113*, 7584–7592.

20 Garand, E.; Wende, T.; Goebbert, D. J.; Bergmann, R.; Meijer, G.; Neumark, D. M.; Asmis, K. R. Infrared Spectroscopy of Hydrated Bicarbonate Anion Clusters: $HCO_3^-(H_2O)_{1-10}$. *J. Am. Chem. Soc.* **2010**, *132*, 849–856.

21 Zhou, J.; Santambrogio, G.; Brümmer, M.; Moore, D. T.; Meijer, G.; Neumark, D. M.; Asmis, K. R. Infrared Spectroscopy of Hydrated Sulfate Dianions. *J. Chem. Phys.* **2006**, *125*, 111102-1–111102-4.

22 Miller, Y.; Chaban, G. M.; Zhou, J.; Asmis, K. R.; Neumark, D. M.; Gerber, R. B. Vibrational Spectroscopy of $(SO_4^{2-})\cdot(H_2O)_n$ Clusters, n = 1–5: Harmonic and Anharmonic Calculations and Experiment. *J. Chem. Phys.* **2007**, *127* (094305), 1–11.

23 Goebbert, D. J.; Wende, T.; Bergmann, R.; Meijer, G.; Asmis, K. R. Messenger-Tagging Electrosprayed Ions: Vibrational Spectroscopy of Suberate Dianions. *J. Phys. Chem. A* **2009**, *113*, 5874–5880.

24 Wende, T.; Wanko, M.; Jiang, L.; Meijer, G.; Asmis, K. R.; Rubio, A.; Spectroscopically Probing Solvent-Mediated Folding in Dicarboxylate Dianions. *Angew. Chem., Int. Ed.* **2011**, *50*, 3807–3810; *Angew. Chem.* **2011**, *123*, 3891–3894.

25 Blades, A. T.; Klassen, J. S.; Kebarle, P. Free-Energies of Hydration in the Gas-Phase of the Anions of Some Oxo Acids of C, N, S, P, Cl, and I. *J. Am. Chem. Soc.* **1995**, *117*, 10563–10571.

26 Wang, X. B.; Nicholas, J. B.; Wang, L. S. Electronic Instability of Isolated SO_4^{2-} and its Solvation Stabilization. *J. Chem. Phys.* **2000**, *113*, 10837–10840.

27 Wang, X. B.; Yang, X.; Nicholas, J. B.; Wang, L. S. Bulk-Like Features in the Photoemission Spectra of Hydrated Doubly Charged Anion Clusters. *Science* **2001**, *294*, 1322–1325.

28 Wang, X. B.; Yang, X.; Wang, L. S. Probing Solution-Phase Species and Chemistry in the Gas Phase. *Int. Rev. Phys. Chem.* **2002**, *21*, 473–498.

29 Bagratashvili, V. N.; Letokhov, V. S.; Makarov, A. A.; Ryabov, E. A. *Multiple Photon Infrared Laser Photophysics and Photochemistry*; Harwood Academic Publishers GmbH: Amsterdam, 1985.

30 Black, J. G.; Yablonovitch, E.; Bloembergen, N.; Mukamel, S. Collisionless Multiphoton Dissociation of SF_6: A Statistical Thermodynamic Process. *Phys. Rev. Lett.* **1977**, *38*, 1131–1134.

31 Goebbert, D. J.; Meijer, G.; Asmis, K. R. 10K Ring Electrode Trap - Tandem Mass Spectrometer for Infrared Spectroscopy of Mass Selected Ions. *AIP Conf. Proc.* **2009**, *1104*, 22–29.

32 Oepts, D.; van der Meer, A. F. G.; van Amersfoort, P. W. The Free-Electron-Laser User Facility Felix. *Infrared Phys. Technol.* **1995**, *36*, 297–308.

33 Asmis, K. R.; Brümmer, M.; Kaposta, C.; Santambrogio, G.; von Helden, G.; Meijer, G.; Rademann, K.; Wöste, L. Mass-Selected Infrared Photodissociation Spectroscopy of $V_4O_{10}^+$. *Phys. Chem. Chem. Phys.* **2002**, *4*, 1101–1104.

34 Relph, R. A.; Bopp, J. C.; Johnson, M. A.; Viggiano, A. A. Argon Cluster-Mediated Isolation and Vibrational Spectra of Peroxy and Nominally D_{3h} Isomers of CO_3^- and NO_3^-. *J. Chem. Phys.* **2008**, *129*, 094303-1–094303-6.

35 Waterland, M. R.; Kelley, A. M. Far-Ultraviolet Resonance Raman Spectroscopy of Nitrate Ion in Solution. *J. Chem. Phys.* **2000**, *113*, 6760–6773.

36 Hudson, P. K.; Schwarz, J.; Baltrusaitis, J.; Gibson, E. R.; Grassian, V. H. A Spectroscopic Study of Atmospherically Relevant Concentrated Aqueous Nitrate Solutions. *J. Phys. Chem. A* **2007**, *111*, 544–548.

37 Xu, M.; Larentzos, J. P.; Roshdy, M.; Criscenti, L. J.; Allen, H. C. Aqueous Divalent Metal-Nitrate Interactions: Hydration Versus Ion Pairing. *Phys. Chem. Chem. Phys.* **2008**, *10*, 4793–4801.

38 Pathak, A. K.; Mukherjee, T.; Maity, D. K. Microhydration of NO_3^-: A Theoretical Study on Structure, Stability and IR Spectra. *J. Phys. Chem. A* **2008**, *112*, 3399–3408.

39 Wang, X. B.; Yang, X.; Wang, L. S.; Nicholas, J. B. Photodetachment and Theoretical Study of Free and Water-Solvated Nitrate Anions, $NO_3^-(H_2O)_n$ (n = 0–6). *J. Chem. Phys.* **2002**, *116*, 561–570.

40 Ramesh, S. G.; Re, S. Y.; Hynes, J. T. Charge Transfer and OH Vibrational Frequency Red Shifts in Nitrate-Water Clusters. *J. Phys. Chem. A* **2008**, *112*, 3391–3398.

41 Miller, Y.; Thomas, J. L.; Kemp, D. D.; Finlayson-Pitts, B. J.; Gordon, M. S.; Tobias, D. J.; Gerber, R. B. Structure of Large Nitrate-Water Clusters at Ambient Temperatures: Simulations with Effective Fragment Potentials and Force Fields with Implications for Atmospheric Chemistry. *J. Phys. Chem. A* **2009**, *113*, 12805–12814.

42 Rudolph, W. W.; Fischer, D.; Irmer, G. Vibrational Spectroscopic Studies and Density Functional Theory Calculations of Speciation in the CO_2-Water System. *Appl. Spectrosc.* **2006**, *60*, 130–144.

43 Max, J. J.; Chapados, C. Isotope Effects in Liquid Water by Infrared Spectroscopy. III. H_2O and D_2O Spectra from 6000 to 0 cm^{-1}. *J. Chem. Phys.* **2009**, *131*, 184505-1–184505-13.

44 Rudolph, W. W.; Irmer, G.; Konigsberger, E. Speciation Studies in Aqueous HCO_3^--CO_3^{2-} Solutions. A Combined Raman Spectroscopic and Thermodynamic Study. *Dalton Trans.* **2008**, 900–908.

45 Nakamoto, K. *Infrared and Raman Spectra of Inorganic and Coordination Compounds*, 5th ed.; Wiley: New York, 1997.

46 Wang, X. B.; Sergeeva, A. P.; Yang, J.; Xing, X. P.; Boldyrev, A. I.; Wang, L. S. Photoelectron Spectroscopy of Cold Hydrated Sulfate Clusters, $SO_4^{2-}(H_2O)_n$ (n = 4–7): Temperature-Dependent Isomer Populations. *J. Phys. Chem. A* **2009**, *113*, 5567–5576.

47 Bush, M. F.; Saykally, R. J.; Williams, E. R. Evidence for Water Rings in the Hexahydrated Sulfate Dianion from IR Spectroscopy. *J. Am. Chem. Soc.* **2007**, *129*, 2220–2221.